Human health risk assessment for nanoparticle-contaminated aquifer systems

Human health risk assessment for aquifer systems at nanoparticle-contaminated sites

Submitted to

Environmental Pollution

Revised manuscript - March 2018

Tiziana Tosco[(1)], Rajandrea Sethi[(1)]*

[(1)] DIATI – Dipartimento di Ingegneria dell'Ambiente, del Territorio e delle Infrastrutture – Politecnico di Torino, C.so Duca degli Abruzzi 24, 10129 Torino, Italy

* Corresponding Author: phone +39 (011) 564 7735; e-mail: rajandrea.sethi@polito.it

Abstract

Nanosized particles (NPs), such as TiO_2, Silver, graphene NPs, nanoscale zero-valent iron, carbon nanotubes, etc., are increasingly used in industrial processes, and releases at production plants and from landfills are likely scenarios for the next years. As a consequence, appropriate procedures and tools to quantify the risks for human health associated to these releases are needed.

The tiered approach of the standard ASTM procedure (ASTM-E2081-00) is today the most applied for human health risk assessment at sites contaminated by chemical substances, but it cannot be directly applied to nanoparticles: NP transport along migration pathways follows mechanisms significantly different from those of chemicals; moreover, and also toxicity indicators (namely, reference dose and slope factor) are NP-specific. In this work a risk assessment approach modified for NPs is proposed, with a specific application at Tier 2 to migration in groundwater. The standard ASTM equations are modified to include NP-specific transport mechanisms. NPs in natural environments are typically characterized by a heterogeneous set of NPs having different size, shape, coating, etc. (all properties having a significant impact on both mobility and toxicity). To take into account this heterogeneity, the proposed approach divides the NP population into classes, each having specific transport and toxicity properties, and simulates them as independent species. The approach is finally applied to a test case simulating the release of heterogeneous Silver NPs from a landfill. The results show that taking into account the size-dependent mobility of the particles provides a more accurate result compared to the direct application of the standard ASTM procedure. In particular, the latter tends to underestimate the overall toxic risk associated to the nP release.

Capsule

A risk assessment procedure for nanoparticle releases at contaminated sites is proposed. The standard human health risk assessment models for subsurface migration are adapted to nanoparticles

1. Introduction

The use of engineered nanoparticles (NPs) in industrial applications and commercial products have grown substantially in recent years. However, despite their great potential for technology, NPs can also represent a significant, and still largely unknown, environmental hazard. NP-containing products are already widely available on the market, or expected to be in few years, likely leading to the dissemination of large amounts of NPs in the environment. Despite the advanced stage of the research on their technological applications, the possible impacts of NPs on the environment are less studied, which may pose concerns on safety as well as social acceptance of NP-based products.

In recent years, a growing body of studies have been devoted to the assessment of potential risks associated to the release of NPs, including the identification of preferential migration pathways, the estimation of NP concentration in the different environmental compartments, and the assessment of their toxicity toward human and ecological targets (Hendren et al., 2013; Garner and Keller, 2014). The majority of these studies focus on the fate of NPs gradually released from diffuse sources, eg. use of NPs-containing fertilizers and sludge in agriculture, direct release from consumer products (eg. paints, textiles, fuels, etc.), and incomplete removal of NPs in wastewater treatment plants (Gottschalk et al., 2009; Batley et al., 2013; Kaegi et al., 2013; Klitzke et al., 2015). A quantitative estimation of potential environmental concentrations of representative NPs from diffuse sources, and the associated toxicity risks, was proposed by several authors. However, comprehensive studies including several NPs and release scenarios are fewer, also due to the extreme complexity of the topic, eg. (Boxall et al., 2007; Hendren et al., 2013; Sun et al., 2014; Dale et al., 2015). The release from diffuse sources is relevant in terms of total mass and accumulation in the environment, but, at the moment, the resulting average NP environmental concentrations are modest, and far below toxicity limits (Batley et al., 2013; Garner and Keller, 2014). Conversely, releases from point sources can result in significantly higher concentrations (and consequently, higher potential risks) at a local scale. Typical release scenarios include leaching from landfills where NPs-containing products are disposed; releases at industrial sites where NPs are manufactured, due to continuous, unintentional losses during normal activities of the plant, or following major accidents which result in the release and consequent accumulation of NPs in the soil and subsoil; long-term re-mobilization of NPs delivered on purpose at contaminated sites for groundwater remediation.

The possible fate of significant amounts of engineered NPs released at point sources, and the associated risk posed to human health, have been scarcely faced by researchers at the moment. To this aim, long-term (chronic) effects could be quantified and evaluated using risk assessment procedures, similar to those conventionally employed in the management of sites contaminated by chemical compounds. The most widely used approach in this sense is the Risk-Based Corrective Action (RBCA) ASTM standard, which quantifies the toxic and carcinogenic risk arising for human receptors due to the exposure to the chemical substances released at contaminated sites (ASTM, 2015). Risk assessment approaches, procedures and computational tools are available and largely used for chemical substances. Extended and modified formulations of the analytical equations of the standard ASTM approach have been recently proposed to incorporate further processes (eg. biodegradation in the unsaturated zone) and tools (eg. sensitivity analysis) (Avagliano et al., 2005; Lemke and Bahrou, 2009; Baciocchi et al., 2010; Verginelli and Baciocchi, 2013). The short- and intermediate-term fate and toxicity of NPs released in major accidents has been recently faced by Nowack et al. (2014) as well as risks associated to the use of NPs as pesticides (Kookana et al., 2014). However, approaches and tools for the estimation of the risk associated to sites contaminated by NPs are almost lacking at the moment: few works were proposed to extend fate models of current risk assessment procedures to nanomaterials (Dale et al., 2014; Praetorius et al., 2014), and a comprehensive approach for the assessment of long-term risks is still missing.

Several challenges are to be faced for a successful adaptation of the ASTM procedure to NPs: on the one hand, particle-specific toxicity parameters (eg. Chronic Reference Dose RfD and Slope Factor SF), requested in the procedure, have been already determined for very few particles; on the other hand, the processes controlling NP migration in the environmental compartments may be significantly different from those associated to chemical substances. Moreover, both mobility and toxicity depend not only on the NP composition, but also on their size, shape, eventual coating, and environmental modifications which particles may undergo after release (eg. oxidation, dissolution, interaction with organic matter, etc.). In particular, a key property which poses major challenges in the adaptation of the ASTM transport models to NPs is particle heterogeneity. Even NPs which are fairly homogeneous when released may significantly change their properties over time, and result in a very heterogeneous population on the long term (Westerhoff and Nowack, 2012). Nanoparticles may be heterogeneous in size, shape, surface coating etc., which are all properties with a significant effect on the NP overall mobility in the subsurface. Among these properties, particle size is definitely a dominant one (Tufenkji and Elimelech, 2004). Particles having the same composition and shape, but different size, are characterized by a different mobility in groundwater.

The toxic effects of nanoparticles have been extensively investigated in recent years, both in vivo and in vitro, but very few toxicity indicators have been determined (Schilling et al., 2010; Shi et al., 2013). Sets of RfD and SF values for particles having the same composition but different size, or coating, are not available in the literature. Moreover, no standard classification of NPs as carcinogenic is available. Ecotoxicity have been quantitatively assessed in some cases for selected nanoparticles (eg. Ag, TiO_2, fullerene, carbon nanotubes), while toxicity limits relevant to human risk assessment have not been standardized yet (Demir et al., 2013; Johnston et al., 2013; Comfort et al., 2014; Siripattanakul-Ratpukdi and Fürhacker, 2014). Values of RfD for Ag NPs have been proposed (Kim et al., 2010; Windler et al., 2013), while in other cases the use of the RfD of the corresponding bulk substances is recommended (Varner et al., 2010).

In this work, the framework for the development of risk assessment procedures for NPs-contaminated sites is presented, discussing the modifications to the standard procedures and mathematical tools already available for chemicals, and the main challenges still to be faced for the application of such a procedure to real contaminated sites. In particular, the crucial role of particle size is discussed, and an adaptation of the standard ASTM procedure at Tier 2 is proposed for NP releases. NP-specific transport models are simplified and adapted to the analytical solutions in the standard ASTM approach, and the selection of appropriate toxicity indicators is briefly discussed. An example of risk assessment for a NP-contaminated site is finally presented.

2. Development of a risk assessment procedure adapted to NPs

The ASTM procedure follows a tiered approach, with complexity increasing from Tier 1 to Tier 3. Tier 1, based on a direct comparison of observed concentrations against screening levels reported in look-up tables, is not site-specific, and is scarcely applied, apart from extremely simplified scenarios. In most cases, a site-specific procedure is adopted, based on the use of analytical or numerical solutions (Tier 2 or 3, respectively) to describe the migration of the contaminants from the source to the potential receptors through different migration pathways. Despite Tier 3 allows for the application of more realistic fate and transport models, Tier 2 is more commonly applied due to the simplicity of use and collectability of the site-specific data required for its application.

Following the ASTM standard (ASTM, 2015), a risk analysis at Tier 2 and 3 is composed by three stages:

- Stage 1, including the identification of the release source and of the relevant migration pathways in the environmental matrices, from the source to the point of exposition (POE) where potential receptors are located.
- Stage 2, including predictive simulation of contaminant spreading along the migration pathways previously identified. Analytical (Tier 2) or numerical (Tier 3) models are applied to quantify the expected concentration at POE (C_{POE}), provided that the concentration at the source (C_0) is known;
- Stage 3, the estimation of the impact on potential receptors in terms of chronic toxicity and carcinogenic effects.

In the next paragraphs, for each stage, the adaptations to extend the ASTM approach to NP-contaminated sites are discussed.

2.1 Stage 1: Major migration pathways for NP release

The ASTM approach is typically applied to contaminated sites. In this case, three major exposure pathways are identified, namely exposure to contaminated soil, contaminated air, and contaminated groundwater. The first is associated to a direct contact of the potential receptor with the contaminated soil; it is therefore limited to on-site exposure, and the definition of migration models is not necessary. Since for most NPs a relatively fast precipitation onto the soil is expected (Garner and Keller, 2014), also migration through air is likely relevant only for on-site exposure.

The subsoil very often represents the most likely migration scenario for the long-term NP fate. Consequently, in this work we focus on this scenario, and NP migration through the air will not be discussed. However, it is worth to mention that, under specific scenarios which may lead to NP dispersion in the air, adequate transport models should be developed and discussed following an approach similar to the one applied here for the subsurface.

2.2 Stage 2: Migration of the NPs from the source to the potential receptors

Particle transport in groundwater is controlled by mechanisms which can only be partially assimilated to those controlling the migration of chemical substances. In the standard ASTM

procedure the migration of a contaminant from the source to the point of exposition of the potential receptor is schematized through the following steps (Figure 1):

- in the source area, the contaminant is dissolved from solid phase into pore water (from S_{soil} to C_{leach}); the process is quantified by the Soil-Water Partition Factor (K_{sw}= S_{soil}/C_{leach}). In case of thick unsaturated zone and/or easily degradable contaminants, additional mitigation processes can be included and modeled at this stage, thus leading to a reduced concentration in the leachate while reaching groundwater (Connor et al., 2007; Verginelli and Baciocchi, 2013).
- When reaching the water table, the leachate mixes with groundwater (from C_{leach} to C_0); the process is quantified by the Leachate Dilution Factor (LDF = C_{leach2}/C_0).
- The contaminant migrates through the aquifer toward the potential receptor (from C_0 to C_{POE}); the process is represented by the Dilution Attenuation Factor (DAF=C_0/C_{POE}).

The first two steps may be included in the so-called Leaching Factor LF=1/(K_{sw}·LDF).

The overall attenuation from the source to the potential receptor is represented by the Natural Attenuation Factor NAF [L^3M^{-1}]:

$$NAF = \frac{S_{soil}}{C_{POE}} = K_{sw} \cdot LDF \cdot DAF \quad (1)$$

where S_{soil} is the contaminant concentration in solid phase at the source, expressed as mass of contaminant per unit mass of soil [MM^{-1}], and C_{POE} is the contaminant concentration in water at POE [ML^{-3}].

At Tier 2, simplified scenarios for contaminant dissolution and transport are adopted, and analytical transport models are applied to predict the concentrations at the potential receptors (C_{POE}). A summary of Tier 2 analytical solutions is reported in Supporting Information. At Tier 3, more complex scenarios can be considered, and numerical solutions are adopted to simulate the migration of the contaminants (Baciocchi et al., 2010; Pinedo et al., 2014; ASTM, 2015).

To take into account the influence of NP heterogeneity (eg. NPs heterogeneous in size) the particle population can be divided into classes, and the transport of each class modeled independently. As a consequence, one value of NAF is to be calculated per each class i, NAF_i:

$$NAF_i = \frac{S_{soil,i}}{C_{POE,i}} = K_{sw,i} \cdot LDF_i \cdot DAF_i \quad (2)$$

Being particle transport class-dependent rather than mass-dependent, it is more convenient to consider number concentrations rather than mass concentrations, thus

$$C_i = m_i N_{w,i} \qquad \text{and} \qquad C = \sum_i m_i N_{w,i} \tag{3a}$$

$$S_i = \frac{1-\varepsilon}{\rho_s} m_i N_{s,i} \qquad \text{and} \qquad S = \frac{1-\varepsilon}{\rho_s} \sum_i m_i N_{s,i} \tag{3b}$$

where $N_{w,i}$ and $N_{s,i}$ are the number concentration of particles of the i-th class per unit volume of water and of solid phase, respectively [L^{-3}], m_i is the mass of a particle of the i-th class [M], ρ_s is the solid matrix bulk density [ML^{-3}], ε is the porosity [-]. The overall mass concentrations for NPs in liquid and solid phase, C and S, can be obtained summing up mass concentrations of the individual classes, C_i and S_i.

Therefore, NAF_i can be defined as

$$NAF_i = \frac{1-\varepsilon}{\rho_s} \frac{N_{s,soil,i}}{N_{w,POE,i}} \tag{4}$$

Similar definitions can be written for $K_{sw,i}$, LDF_i and DAF_i (Supporting Information).

2.2.1 Definition of DAF for nanoparticles

In the standard ASTM procedure, the spreading of chemical substances in groundwater (and consequently NAF) is quantified by analytical or numerical models describing the contaminant transport due to advection, dispersion, sorption onto the solid matrix, degradation, and volatilization. Assuming first order degradation/volatilization and linear equilibrium sorption, the partial differential equation (PDE) describing the solute transport in groundwater is:

$$\frac{\partial}{\partial t}(\varepsilon R C) + \nabla \cdot (uC) - \nabla \cdot (\varepsilon D \nabla C) + \varepsilon \lambda C = 0 \tag{5}$$

where u is the specific discharge rate [LT^{-1}], D is the hydrodynamic dispersion tensor [L^2T^{-1}], λ is the first order degradation rate constant (describing either chemical degradation, biodegradation or volatilization) [T^{-1}], and R is the retardation factor (describing linear equilibrium sorption onto the porous matrix). At Tier 2, the ASTM procedure suggests the use of the analytical solution of

Domenico (Domenico, 1987) for the calculation of C_{POE}. In particular, the solution at steady state is usually adopted:

$$\frac{C_{POE}}{C_0} = \frac{1}{4}\exp\left[\left(\frac{x}{2\alpha_x}\right)\left(1-\sqrt{1+\frac{4\lambda\alpha_x}{v}}\right)\right]\cdot\left[erf\left(\frac{y+\frac{L_w}{2}}{2\sqrt{\alpha_y x}}\right)-erf\left(\frac{y-\frac{L_w}{2}}{2\sqrt{\alpha_y x}}\right)\right]\cdot\left[erf\left(\frac{z+\delta_{sw}}{2\sqrt{\alpha_z x}}\right)-erf\left(\frac{z-\delta_{sw}}{2\sqrt{\alpha_z x}}\right)\right] \quad (6)$$

where v is the seepage velocity u/ε [LT^{-1}], L_w and δ_{sw} are the transversal and vertical extents of the contamination source (Figure 1) [L], α_x α_y and α_z are the horizontal, transversal and vertical dispersivities [L]. The Domenico transient solution is reported in the Supporting Information.

Two major points can be identified which make the direct application of Eq. 5 (and its analytical or numerical solutions) inappropriate to NPs as it is. These two aspects are the influence of heterogeneities within the NP population (above all, the heterogeneity in size), and the intrinsic difference of the mechanisms controlling the NP interactions with the porous medium, compared to solutes. The first aspect can be taken into account by dividing the NP population into classes, with different transport properties, and consequently calculating NAF_i per each class, as defined in Eq. 2. Concerning the second aspect, NP fate in the subsoil follows mechanisms noticeably different from those typical of solutes. Particle transport is controlled by advection, dispersion and kinetic mass transfer between liquid and solid phase (attachment/detachment) (Kretzschmar et al., 1999; Tosco et al., 2009). Mechanical filtration of large particles or aggregates may also play a relevant role. In unsaturated soils, particle attachment at the air-water interface can also have a significant impact (Sim and Chrysikopoulos, 1999; Bradford and Torkzaban, 2008). A vast literature is available on the different processes and the corresponding mathematical formulations (Johnson et al., 1996; Bradford et al., 2002; Johnson et al., 2007; Petosa et al., 2010; Messina et al., 2015), and a review of the topic is beyond the purpose of this paper.

Considering the transport mechanisms led by Eq. 5, some are clearly inapplicable to NPs, eg. the contaminant volatilization. Also NP biodegradation is unlikely: bacteria-mediated transformations are expected for most NPs, but their effect is a modification of surface properties and transport behavior, rather than a "disappearance" of the particles (Lowry et al., 2012; Nowack et al., 2012; Schaumann et al., 2015). Moreover, the equilibrium sorption of a solute can only be partly assimilated to the kinetic deposition and release of NPs, as widely debated in the recent literature (Dale et al., 2014; Praetorius et al., 2014; Cornelis, 2015). As a consequence, the transport models adopted in the standard ASTM procedure cannot be directly applied to simulate the transport of

NPs, but must be adapted and extended to include NP-relevant mechanisms of transport. Neglecting NP aggregation and/or breakage of aggregates, the model equation for the i-th class of NPs is

$$\frac{\partial}{\partial t}\left(\varepsilon N_{w,i}\right)+\frac{\partial}{\partial t}\left[(1-\varepsilon)N_{s,i}\right]+\nabla\cdot\left(uN_{w,i}\right)-\nabla\cdot\left(\varepsilon D\nabla N_{w,i}\right)=0 \qquad (7)$$

The second term of Eq. 7 represents the interactions of the suspended NPs with the porous matrix, and can be expressed, in a general form, as

$$\frac{\partial}{\partial t}\left[(1-\varepsilon)N_{s,i}\right]=\varepsilon k_{a,i}\psi_i N_{w,i}-k_{d,i}(1-\varepsilon)N_{s,i} \qquad (8)$$

where $k_{a,i}$ and $k_{d,i}$ are respectively the attachment and detachment rates [T^{-1}] of the i-th class, and ψ_i is a kinetic function depending on the specific attachment mechanism (linear deposition, blocking, ripening, straining...). The three parameters all depend on particle size.

An analytical solution to Eqs. 7-8 for 3D domains, equivalent to the Domenico's solution, is not available. Analytical solutions were developed for 1D domains (Šimůnek et al., 2008) and for simplified 3D (Sim and Chrysikopoulos, 1998), but for general 3D domains numerical solutions are requested, eg. MNM3D (Bianco et al., 2016). Even if such models can provide an accurate and physically meaningful description of particle transport processes, they are too complex for a direct application at Tier 2. For this reason, we propose here an adaptation of Domenico's analytical solution to solve Eqs. 7-8, for each class of NPs i, to simulate NP transport in 3D scenarios suitable for a Tier 2 risk analysis.

To this aim, Eqs. 7-8 must be first re-arranged to the structure of Eq. 5 (Table 1). For example, comparing Eqs. 7-8 to Eq. 5, it can be observed that linear irreversible attachment (ψ_i=1, $k_{d,i}$=0 in Eq. 8) can be formally simulated as a first order degradation without any simplifying assumption. Conversely, NP deposition/release can be approximated as a sorption process only for those formulations leading to a dynamic equilibrium between solid and liquid phase (eg. blocking, linear reversible deposition), and only under specific simplifying assumptions.

From a formal point of view, a dynamic equilibrium is possible when Eq. 7 can be re-arranged in the form of an implicit kinetic formulation (Azizian, 2004):

$$\frac{\partial}{\partial t}\left[(1-\varepsilon)N_{s,i}\right]=K_{eq,i}\left(N^{*}_{s,i}-N_{s,i}\right) \qquad (9)$$

where $N_{s,i}^*$ [-] is the NP concentration in the solid phase when the dynamic balance is reached, and $K_{eq,i}$ [$ML^{-3}T^{-1}$] is the implicit rate constant. Both $N_{s,i}^*$ and $K_{eq,i}$ depend on the considered deposition/release mechanism.

If Eq. 9 can be written, a retardation factor can be formally defined as:

$$R_i = 1 + \frac{1-\varepsilon}{\varepsilon}\frac{N_{s,i}^*}{N_w} \qquad (10)$$

The approximation of dynamic equilibrium, and therefore the applicability of a retardation factor, is valid when the characteristic time of the attachment/detachment process is significantly lower than the characteristic time of advection. Similarly to solute sorption (Azizian, 2004; Werner et al., 2012), also for NPs it is possible to evaluate how far conditions are from equilibrium by means of the Damköler number:

$$Da_i = \frac{K_{eq,i} L}{u} \qquad (11)$$

where L is the scale of the problem (here, the x coordinate). Kinetic processes can be neglected for Da>1.

From a practical point of view, equilibrium is established and NP deposition can be approximated by a retardation factor when Da>1, that is for $L > u/(1-\varepsilon)k_{d2}$.

If a particle size distribution is considered, R_i is to be defined per each class. A summary of the values of λ_i and R_i for the most common deposition kinetics is provided in Table 1. Details on the applicability of this approximation, and a step-by-step procedure for the selection of the appropriate approximation are provided in the Supporting Information.

In conclusion, it is strongly recommended that, when developing a comprehensive NP risk assessment tool (likely, at Tier 3), the impact of a heterogeneous NP population is included in the transport and fate models, namely using solutions to Eqs. 7-8 for a heterogeneous NP population with class-dependent parameters, rather than using a homogeneous one. Nevertheless, for a first screening, at Tier 2 simplifying assumptions can be made concerning NP transport on the long term and over large scales, and consequently the mathematical formulation adopted in standard ASTM at Tier 2 (i.e. using Eq. 6) can be adopted also for NPs without major modifications (see Paragraph 3).

2.3 Stage 3: risk estimate

The standard ASTM procedure quantifies the risk associated to the chronic exposure to a contaminant or, as in this case, to nanoparticles, through two indexes, namely the Hazard Quotient (HQ) for toxic effects, and the Incremental Lifetime Cancer Risk (ILCR) for carcinogenic effects. The two indexes cumulate the chronic effects generated by the different exposure pathways and substances (ASTM, 2015).

For a single substance and for the exposure due to injection of groundwater, the HQ index is calculated as the ratio of the average intake of substance at POE, and the Reference Dose:

$$HQ = \frac{C_{POE} \cdot E}{RfD} \tag{12}$$

where E is the exposure rate (i.e. average amount of water ingested per day per unit body weight) [$L^3M^{-1}T^{-1}$] and RfD is the Reference Dose [$L^3M^{-1}T^{-1}$], that is the maximum dose below which no chronic toxic effect is observed (Connor et al., 2007; ASTM, 2015). RfD values are typically defined from NOAEL (Not Observed Adverse Effect Level) or LOAEL (Lowest Observed Adverse Effects Level), and standardized in databases, eg. RAIS (http://rais.ornl.gov/tutorials/toxvals.html). HQ<1 corresponds to an acceptable toxic risk, HQ>1 to an unacceptable toxic risk.

For carcinogenic effects, the ILCR index is calculated as the product of the average intake $C_{POE} \cdot E$ and the Slope Factor SF [-], determined from dose-response curves:

$$ILCR = C_{POE} \cdot E \cdot SF \tag{13}$$

Figure 2 reports a comparison of different scenarios for the calculation of the toxic effects of NPs, assuming different approximations. Scenario A corresponds to the standard ASTM procedure for chemical substances: transport models describe how the NP concentration decreases from the source to the POE, without taking into account any NP-dependent transport parameter. In this case Eq. 12 is applied to calculate the HQ index using a constant value of RfD. However, this approach is too simplistic, and size-dependent transport of the NPs from the source to POE must be considered (Scenario B). As evidenced in Figure 2, taking into account the NP size-dependent transport may result in significantly different values of HQ, even if the same NP mass at source is considered.

Both in the case of application of the (simplistic) Scenario A, and of Scenario B, the definition of RfD (and SF) values appropriate for NPs is likely the major challenge for the implementation of the

risk assessment procedure. Similarly to NP transport, also NP toxicity is known to be size dependent. Toxicity studies on silver NPs provided different values of RfD for particles of different size, particularly, higher toxicity for smaller particles (Kim et al., 2010; Windler et al., 2013; Hadrup and Lam, 2014). Also the eventual coating may affect NPs toxicity: coating by humic acid is reported to decrease toxicity of Silver NPs, while coating with citrate increases toxicity (Angel et al., 2013).

Size-dependent toxicity profiles would be crucial for the correct application of risk assessment to NPs. As reported for Scenario C in Figure 2, considering size-dependent RfD values, HQ may be significantly different from the values obtained in Scenarios A and B. If size-dependent toxicity values for NPs were available, a rigorous approach for the calculation of HQ and ILCR should take into consideration the particle size distribution at POE, and the toxicity indexes should be obtained by combining Eqs. 7-8 with Eqs. 12-13:

$$HQ = \sum_i \left(\frac{C_{POE,i}}{RfD_i} \right) \cdot E = \sum_i \left(\frac{m_i \cdot N_{w,POE,i}}{RfD_i} \right) \cdot E \quad (14)$$

$$ILCR = \sum_i \left(C_{POE,i} \cdot SF_i \right) \cdot E = \sum_i \left(m_i \cdot N_{w,POE,i} \cdot SF_i \right) \cdot E \quad (15)$$

Finally, the possible particle dissolution in the human body may also be an additional challenge when evaluating NP-related risk to human health: for eg., some particles (eg. Silver NPs) may be partly dissolved when ingested. For this reason, it would be recommended to calculate the risk associated to ingestion using both the limits for NPs, and the limits for the corresponding dissolved species.

3. Application of the NP-modified risk assessment procedure

3.1 Methods

The risk assessment procedure described in paragraph 2 was applied to a synthetic case of release of Silver nanoparticles (Ag-NPs) from a landfill. The application followed these steps:

- Laboratory results from a published work on Ag-NP transport (Wang et al., 2014) were considered, and NP transport parameters were obtained by least-squares fitting the experimental breakthrough curves;
- The dependency of NP transport parameters on flow velocity and particle size was modeled following the approach of a previous work (Tosco et al., 2014) and transport parameters for the synthetic landfill test case were obtained from column test results; transport mechanisms were approximated to degradation and sorption processes, as discussed in paragraph 2.2;
- NP release from the landfill and transport in groundwater was simulated under Scenarios A and B of Figure 2 and toxic risk was estimated.

3.1.1 Column tests

Experimental results of column transport tests of Ag-NPs (average size d_p=16 nm) in natural soils reported by Wang et al. (2014), were modeled. In particular, two experimental breakthrough curves (BTCs) for Ag-NPs injected in pure quartz sand, and a mixture of 20% quartz sand and 80% of natural soil (average size d_s=0.65 mm for both quartz sand and soil) were considered, herein named "0%Soil" and "80%Soil", respectively. The NPs were injected at a concentration of 100 mg/l in fully saturated columns (inner diameter 1.1 cm, column length 10 cm, discharge rate 0.25 ml/min, porosity 0.42). The BTCs were inverse-fitted using the software MNMs (www.polito.it/groundwater/software/MNMs) (Tosco and Sethi, 2009; Bianco et al., 2016). Two linear interaction sites were considered, one irreversible (fitted parameter: $k_{a,irr}$) and one reversible (fitted parameters: $k_{a,rev}$ and $k_{d,rev}$). Thus Eqs. 7-8 become

$$\begin{cases} \frac{\partial}{\partial t}\left(\varepsilon N_{w,i}\right)+\frac{\partial}{\partial t}\left[(1-\varepsilon)N_{s,irr,i}\right]+\frac{\partial}{\partial t}\left[(1-\varepsilon)N_{s,rev,i}\right]+\nabla\cdot\left(uN_{w,i}\right)-\nabla\cdot\left(\varepsilon D\nabla N_{w,i}\right)=0 \\ \frac{\partial}{\partial t}\left[(1-\varepsilon)N_{s,irr,i}\right]=\varepsilon k_{a,irr,i}N_{w,i} \\ \frac{\partial}{\partial t}\left[(1-\varepsilon)N_{s,rev,i}\right]=\varepsilon k_{a,rev,i}N_{w,i}-k_{d,rev,i}(1-\varepsilon)N_{s,rev,i} \end{cases} \quad (16)$$

For the column tests, particles were assumed mono-dispersed and consequently only one class of NP size was considered (i=1). For the simulation of the release from the landfill, 20 classes were considered in Scenario B (i=1,...,20).

3.1.2 Modeling attachment/detachment parameters

An approach similar to Tosco et al. (2014) was adopted to model the dependency of $k_{a,irr,i}$ and $k_{a,rev,i}$ from particle size and flow velocity. Briefly, the attachment rate is assumed proportional to the flow velocity v and the deposition efficiency η_0:

$$k_{a,i} = A_i v \eta_{0,i} \quad (17)$$

where A_j is an empirical coefficient which incorporates dependences on other parameters [L^{-1}].

The Yao model (Yao et al., 1971) was used to calculate $\eta_{0,i}$, which is function of several parameters, including v and particle size.

Also the detachment rate depends on flow velocity (Tosco et al., 2014), thus

$$k_{d,i} = B_i v \quad (18)$$

3.1.3 Synthetic test case of Ag-NP release from a landfill

A landfill of longitudinal size W=80 m and transverse size L_{gw}=80 m subject to effective recharge I_{eff}=450 mm/y was considered. The landfill is located above a 15 m thick unconfined aquifer, with effective porosity ε=0.2, Darcy velocity $u=7.6\cdot10^{-7}$ m/s, longitudinal, transversal and vertical dispersivities (α_x, α_y, α_z) equal to 10, 3.3 and 0.5 m respectively. The concentration of NPs in landfill waste and leachate may significantly vary among sites (Gottschalk et al., 2009; Sun et al., 2014). In this work, C_{leach}=15 mg/l was assumed as representative value (Yang et al., 2012). No attenuation was considered in the unsaturated zone for cautionary purposes, and only mixing with groundwater (Eqs. S.3-S.4 in SI) was considered to obtain C_0.

Exposure E= 0.027 l/kg/d was used following the ASTM standard, corresponding to residential use. RfD was assumed constant for all particle classes, equal to $3.0\cdot10^{-2}$ mg/kg/d, based on the work of Kim et al. (Kim et al., 2010).

3.2. Results and Discussion

3.2.1 NP transport parameters: from column tests to simulated landfill release

The experimental data of Wang et al. (2014) were first modeled using the dual site linear attachment/detachment of Eq. 16 with i=1 (Figure 3 and Table 2). The two interactions mechanisms (linear irreversible attachment and linear reversible attachment) were selected following a stepwise approach, starting from the simplest model and increasing its complexity (and consequently number of fitted parameters) until a satisfactory fitting of the experimental data was obtained. Briefly, the simplest case of one linear irreversible interaction site (1 fitted parameter per each test, $k_{a,irr}$) was considered the first option for both tests. However, the fitting was not satisfactory (data not reported). The same for one linear reversible site (2 fitted parameters, $k_{a,rev}$ and $k_{d,rev}$). The third option, namely linear irreversible attached associated to a second site of linear irreversible attachment (3 parameters: $k_{a,irr}$, $k_{a,rev}$ and $k_{d,rev}$) was the simplest providing a good fitting, with R^2 parameter equal to 0.9888 and 0.8693 was obtained respectively for 0%Soil and 80%Soil. The fitted attachment rate k_{airr} for the first deposition mechanism (linear irreversible) is the same for both column tests, while $k_{a,rev}$ and $k_{d,rev}$ for the second deposition mechanism (linear reversible) are different. From a physical point of view, this finding suggests that irreversible attachment was not affected by soil composition, but only by particle and soil size (and flow rate), and is therefore likely related to NP mechanical retention. Conversely, reversible attachment also depends on soil composition.

Eq. 17 was applied to fitted $k_{a,irr}$ and $k_{a,rev}$, Eq. 18 to fitted $k_{d,rev}$ obtained to determine the three parameters A_{irr}, A_{rev} and B_{rev}. It is worth to mention that in the presence of linear (reversible or irreversible) deposition, the attachment rate is independent of the injected concentration. As a consequence, the parameters determined from these column tests (performed injecting Silver NPs at a concentration of 100 mg/l) can be assumed valid for the simulation of the leaching landfill, where the NP released concentration is 15 mg/l.

Two alternative approaches were then considered to simulate NP release from the landfill, among those reported in Figure 2:

- Scenario A: NP size distribution was not considered; the released NPs are a homogeneous samples of Silver NPs having the same size as those of the column tests (i.e. 16 nm);

- Scenario B: An NP size distribution was assumed, in the range 5 to 200 nm, divided into 20 classes, with same average particle size of Scenario A (16 nm). The particle size distribution is reported in Figure 6 (blue curve at the source, i.e. X = 0).

In both Scenarios, the same mass of particles (15 g/l) was released.

The attachment and detachment rates ($k_{a,irr}$, $k_{a,rev}$ and $k_{d,rev}$) for the two Scenarios were calculated using the values of A_{irr}, A_{rev} and B_{rev} (obtained from the column tests) in Eqs. 17-18. Following the Yao model, the deposition efficiency (Figure 6), and consequently k_a, is a function, among other parameters, of particle size and flow velocity; following Eq. 18, k_d is independent of particle size, and is affected only by flow velocity. Consequently, for Scenario A, $k_{a,irr}$, $k_{a,rev}$ and $k_{d,rev}$ are constant parameters, and the only difference compared to the column tests is due only to the different flow velocity of the aquifer compared to the one applied in the column tests. For Scenario B, a different set of $k_{a,irr,i}$ and $k_{a,rev,i}$ is obtained for each class, while $k_{d,red}$ is constant for all classes.

The coefficients for both Scenarios are reported in Table 2.

Compared to the parameters fitted for column tests, the values obtained for Scenarios A and B for the landfill synthetic case are roughly one order of magnitude lower, due to the different flow velocity of column tests ($u=4.3\cdot10^{-5}$ m/s) and the landfill case ($u=7.6\cdot10^{-7}$ m/s). Also particle size significantly influences the attachment/detachment coefficients: for Scenario B, $k_{a,irr,i}$ and $k_{a,rev,i}$ span over at least one order of magnitude, with particle size ranging from 15 to 200 nm, with evident implications on the relevance of considering particle size distribution when simulating NP transport (paragraph 2.2.1). These two findings both suggest the importance of considering appropriate models and experimental conditions for the determination of NP transport parameters: if a risk analysis for an NP release from a landfill similar to this test case is to be performed, it is crucial to determine particle transport parameters from experiments performed as close as possible to the real site conditions (eg. flow velocity and NP type and size). If such conditions cannot be reproduced in the laboratory, appropriate, well-established relationships like those of Eqs. 17-18 are to be applied to transfer the NP parameters to the field scale conditions.

3.2.2 NP risk assessment

The Domenico solution was then applied for the calculation of C_{POE} for the Ag-NPs in both Scenarios A and B, and the modified ASTM procedure was applied for the risk assessment (procedure fully described in SI in paragraph S2). The vertical extent of the mixing zone in the

aquifer (δ_{gw}) was calculated using Eq. S.4, resulting equal to 16.3 m (higher than the saturated thickness b). As a consequence it was assumed δ_{gw}=b and vertical dispersion was neglected (Connor et al., 2007). Mixing of leachate with groundwater resulted in a dissolved concentration at source C_0=3.08 mg/l.

Applying the approximations discussed in paragraph 2.2.1, for both Scenarios A and B irreversible deposition was simulated as a first order degradation, reversible deposition as a linear sorption. The corresponding λ_i and R_i were calculated using the equations reported in Table 1 and are reported in Table 2. The applicability of this approximation was verified using Eq. 11. For both Scenarios, Da>1 is verified for any x>8.2 cm, thus allowing the application of Domenico's solution all over the domain.

Transport in groundwater was simulated for Scenarios A and B in both transient and steady state conditions to calculate the C_{POE} along the axis (y=0, z=0) where the highest concentrations are found (Figure 4). Provided that the same concentration of Silver NPs is released at the source, under Scenario A particles travel for a shorter distance: compare, for example, the concentration profiles (left y-axis) along the plume axis at steady state in Figure 4 (to allow comparison of the two Scenarios, the total mass concentration is here calculated for Scenario B using Eq. 3a). This observed difference is due to the higher attachment efficiency, and consequently attachment rate, characterizing 16 nm particles when compared to larger ones, which are present in the population of Scenario B (see η_0 trend in Figure 6). Conversely, for Scenario B, particles as a whole travel for longer distances, due to the presence of (few) larger particles having a lower attachment efficiency.

These observations have a direct impact on the results in terms of toxic risk. For Scenario A, Eq. 12 was directly applied to calculate HQ, since only one class of particles was considered. For Scenario B, the Domenico solution was applied independently for each NP class, and Eq. 14 was then used to calculate HQ, assuming that RfD is the same for all classes. HQ values along the x-axis are reported in Figure 4. Being the retardation factor R higher for 80%Soil than for 10%Soil, in transient conditions (namely, 5 years after the initial release from the landfill) the extent of the area with HQ above the threshold limit of 1 is significantly higher for the 0%Soil, as it can be observed from both concentration profiles along the plume axis (Figure 4), maps (Figure 5) and numerical values of length and area with HQ>1 (Table S.1 in SI). However, the HQ at the steady state, which is usually considered for risk assessment, is the same for both 0%Soil and 80%Soil, since the irreversible attachment coefficient, and consequently the parameter λ, is the same, and the retardation coefficient R has no influence on the steady state concentration (see paragraph A.2).

The results evidence that for Scenario B the overall mobility of the Ag-NP is higher, thus resulting in larger areas where HQ>1. For example, at steady state, HQ values higher than 1 are found up to 85.6 m for Scenario A and 98.2 m for Scenario B downgradient the source of contamination (Figure 5 and Table S.1). Correspondingly, the area having HQ>1 is 16% larger for Scenario B compared to Scenario A. This is due to the different transport of different classes of NPs, which are characterized by different values of k_{aj}: the attachment efficiency (Figure 6) is higher for smaller particles, lower for larger particles. As a consequence, larger particles travel for longer distances, and the original particle size distribution at source (blue line in Figure 6) changes its shape along the x-axis, showing a more pronounced decrease in the concentration of smaller particles compared to larger ones. These results confirm that the adoption of size-dependent transport equations for NPs is worth to be applied, even in a simplified Tier 2 approach, and that the direct application of Scenario A is too simplistic.

4. Conclusions

The ASTM approach for the Tier 2 risk assessment procedure for contaminated sites has been here adapted for application of releases of nanoparticles, and an example application to landfill leachate was presented. Even if particle transport in porous media is a complex phenomenon, the governing equations can be simplified under reasonable assumptions. It was demonstrated that particle transport described by a combination of a linear reversible and a linear irreversible attachment can be solved using the same equations of the transport of a dissolved contaminant subject to first order degradation rate and linear sorption, provided that the time scale of the dynamic attachment/detachment process is significantly smaller than the time scale of the transport in the porous medium. Moreover, it was demonstrated that considering the size-dependent transport of heterogeneous populations of NPs may lead to results, in terms of HQ values at POE, significantly different compared to the simplistic model where the particle size dependent transport is not considered. Similar considerations can be applied for other particle properties, eg. shape, surface coating, etc., which have an impact on NP mobility in the subsoil, and the risk assessment procedure for these cases could be the same here discussed for size-dependent particle transport.

Nevertheless, very few data are available at the moment on the influence of NP size, coating, shape etc. on their toxicity (particularly, chronic toxicity, requested in risk analysis). This represents the

great challenge to the application of a risk assessment procedure to sites contaminated by engineered nanoparticles. In this sense, the availability of size-dependent (or, more in general parameter-dependent) reference doses is an unavoidable necessity, which has not been addressed at the moment.

It is finally worth to mention that the standard ASTM procedure do not take into account particles retained on the soil. However, it cannot be excluded that such NPs can be re-mobilized on a long term (Navarro et al., 2014), following for eg. changes in groundwater hydrochemical conditions. As a consequence, it is recommended that this issue is evaluated when dealing with sites contaminated by NPs, and the possible release of deposited NPs on a long time scale is carefully evaluated and eventually included in risk assessment scenarios.

Acknowledgement

The authors thank Mr. Federico Mondino for the collaboration in reviewing the literature on NP toxicity. This research did not receive any specific grant from funding agencies in the public, commercial, or not-for-profit sectors

References

Angel, B.M., Batley, G.E., Jarolimek, C.V. and Rogers, N.J., 2013. The impact of size on the fate and toxicity of nanoparticulate silver in aquatic systems. Chemosphere, 93(2): 359-365.

ASTM, 2015. Standard Guide for Risk-Based Corrective Action - ASTM-E2081-00, ASTM International, West Conshohocken, PA, 2015, www.astm.org.

Avagliano, S., Vecchio, A. and Belgiorno, V., 2005. Sensitive parameters in predicting exposure contaminants concentration in a risk assessment process. Environmental Monitoring and Assessment, 111(1-3): 133-148.

Azizian, S., 2004. Kinetic models of sorption: a theoretical analysis. Journal of Colloid and Interface Science, 276(1): 47-52.

Baciocchi, R., Berardi, S. and Verginelli, I., 2010. Human health risk assessment: Models for predicting the effective exposure duration of on-site receptors exposed to contaminated groundwater. Journal of Hazardous Materials, 181(1–3): 226-233.

Batley, G.E., Kirby, J.K. and McLaughlin, M.J., 2013. Fate and risks of nanomaterials in aquatic and terrestrial environments. Accounts of Chemical Research, 46(3): 854-862.

Bianco, C., Tosco, T. and Sethi, R., 2016. A 3-dimensional micro- and nanoparticle transport and filtration model (MNM3D) applied to the migration of carbon-based nanomaterials in porous media. Journal of Contaminant Hydrology, 193: 10-20.

Boxall, A.B.A., Tiede, K. and Chaudhry, Q., 2007. Engineered nanomaterials in soils and water: How do they behave and could they pose a risk to human health? Nanomedicine, 2(6): 919-927.

Bradford, S.A., Yates, S.R., Bettahar, M. and Simunek, J., 2002. Physical factors affecting the transport and fate of colloids in saturated porous media. Water Resources Research, 38(12): 631-6312.

Bradford, S.A. and Torkzaban, S., 2008. Colloid transport and retention in unsaturated porous media: A review of interface-, collector-, and pore-scale processes and models. Vadose Zone Journal, 7(2): 667-681.

Comfort, K.K., Braydich-Stolle, L.K., Maurer, E.I. and Hussain, S.M., 2014. Less is more: Long-term in vitro exposure to low levels of silver nanoparticles provides new insights for nanomaterial evaluation. ACS Nano, 8(4): 3260-3271.

Connor, J.A., Bowers, R.L., McHugh, T.E. and Spexet, A.H., 2007. RBCA Tool Kit for Chemical Releases. Software Guidance Manual, Groundwater Services, Inc., Houston, Texas.

Cornelis, G., 2015. Fate descriptors for engineered nanoparticles: the good, the bad, and the ugly. Environmental Science: Nano, 2(1): 19-26.

Dale, A., Casman, E.A., Lowry, G.V., Lead, J.R., Viparelli, E. and Baalousha, M.A., 2015. Modeling nanomaterial environmental fate in aquatic systems. Environmental Science & Technology.

Dale, A.L., Lowry, G.V. and Casman, E., 2014. Much ado about [small alpha]: Reframing the debate over appropriate fate descriptors in nanoparticle environmental risk modeling. Environmental Science: Nano.

Demir, E., Turna, F., Vales, G., Kaya, B., Creus, A. and Marcos, R., 2013. In vivo genotoxicity assessment of titanium, zirconium and aluminium nanoparticles, and their microparticulated forms, in Drosophila. Chemosphere, 93(10): 2304-2310.

Domenico, P.A., 1987. An analytical model for multidimensional transport of a decaying contaminant species. Journal of Hydrology, 91(1): 49-58.

Garner, K.L. and Keller, A.A., 2014. Emerging patterns for engineered nanomaterials in the environment: A review of fate and toxicity studies. Journal of Nanoparticle Research, 16(8).

607 Gottschalk, F., Sonderer, T., Scholz, R.W. and Nowack, B., 2009. Modeled Environmental
608 Concentrations of Engineered Nanomaterials (TiO2, ZnO, Ag, CNT, Fullerenes) for
609 Different Regions. Environmental Science & Technology, 43(24): 9216-9222.
610 Hadrup, N. and Lam, H.R., 2014. Oral toxicity of silver ions, silver nanoparticles and colloidal
611 silver - A review. Regulatory Toxicology and Pharmacology, 68(1): 1-7.
612 Hendren, C.O., Lowry, M., Grieger, K.D., Money, E.S., Johnston, J.M., Wiesner, M.R. and
613 Beaulieu, S.M., 2013. Modeling approaches for characterizing and evaluating environmental
614 exposure to engineered nanomaterials in support of risk-based decision making.
615 Environmental Science and Technology, 47(3): 1190-1205.
616 Johnson, P.R., Sun, N. and Elimelech, M., 1996. Colloid transport in geochemically heterogeneous
617 porous media: Modeling and measurements. Environmental Science and Technology,
618 30(11): 3284-3293.
619 Johnson, W.P., Li, X. and Yal, G., 2007. Colloid retention in porous media: Mechanistic
620 confirmation of wedging and retention in zones of flow stagnation. Environmental Science
621 and Technology, 41(4): 1279-1287.
622 Johnston, H. et al., 2013. Engineered nanomaterial risk. Lessons learnt from completed
623 nanotoxicology studies: Potential solutions to current and future challenges. Critical
624 Reviews in Toxicology, 43(1): 1-20.
625 Kaegi, R., Voegelin, A., Ort, C., Sinnet, B., Thalmann, B., Krismer, J., Hagendorfer, H., Elumelu,
626 M. and Mueller, E., 2013. Fate and transformation of silver nanoparticles in urban
627 wastewater systems. Water Research, 47(12): 3866-3877.
628 Kim, Y., Song, M., Park, J., Song, K., Ryu, H., Chung, Y., Chang, H., Lee, J., Oh, K., Kelman, B.,
629 Hwang, I. and Yu, I., 2010. Subchronic oral toxicity of silver nanoparticles. Particle and
630 Fibre Toxicology, 7(1): 20.
631 Klitzke, S., Metreveli, G., Peters, A., Schaumann, G.E. and Lang, F., 2015. The fate of silver
632 nanoparticles in soil solution — Sorption of solutes and aggregation. Science of The Total
633 Environment(in press).
634 Kookana, R.S. et al., 2014. Nanopesticides: Guiding Principles for Regulatory Evaluation of
635 Environmental Risks. Journal of Agricultural and Food Chemistry, 62(19): 4227-4240.
636 Kretzschmar, R., Borkovec, M., Grolimund, D. and Elimelech, M., 1999. Mobile subsurface
637 colloids and their role in contaminant transport. Advances in Agronomy, Vol 66, 66: 121-
638 193.
639 Lemke, L.D. and Bahrou, A.S., 2009. Partitioned multiobjective risk modeling of carcinogenic
640 compounds in groundwater. Stochastic Environmental Research and Risk Assessment,
641 23(1): 27-39.
642 Lowry, G.V., Gregory, K.B., Apte, S.C. and Lead, J.R., 2012. Transformations of Nanomaterials in
643 the Environment. Environmental Science & Technology, 46(13): 6893-6899.
644 Messina, F., Marchisio, D.L. and Sethi, R., 2015. An extended and total flux normalized correlation
645 equation for predicting single-collector efficiency. Journal of Colloid and Interface Science,
646 446: 185-193.
647 Navarro, D.A., Kirby, J.K., McLaughlin, M.J., Waddington, L. and Kookana, R.S., 2014.
648 Remobilisation of silver and silver sulphide nanoparticles in soils. Environmental Pollution,
649 193: 102-110.
650 Nowack, B., Ranville, J.F., Diamond, S., Gallego-Urrea, J.A., Metcalfe, C., Rose, J., Horne, N.,
651 Koelmans, A.A. and Klaine, S.J., 2012. Potential scenarios for nanomaterial release and
652 subsequent alteration in the environment. Environmental Toxicology and Chemistry, 31(1):
653 50-59.
654 Nowack, B., Mueller, N., Krug, H. and Wick, P., 2014. How to consider engineered nanomaterials
655 in major accident regulations? Environmental Sciences Europe, 26(1): 2.

656 Petosa, A.R., Jaisi, D.P., Quevedo, I.R., Elimelech, M. and Tufenkji, N., 2010. Aggregation and
657 Deposition of Engineered Nanomaterials in Aquatic Environments: Role of
658 Physicochemical Interactions. Environmental Science & Technology, 44(17): 6532-6549.
659 Pinedo, J., Ibáñez, R. and Irabien, Á., 2014. A comparison of models for assessing human risks of
660 petroleum hydrocarbons in polluted soils. Environmental Modelling & Software, 55(0): 61-
661 69.
662 Praetorius, A., Tufenkji, N., Goss, K.-U., Scheringer, M., von der Kammer, F. and Elimelech, M.,
663 2014. The road to nowhere: equilibrium partition coefficients for nanoparticles.
664 Environmental Science: Nano, 1(4): 317-323.
665 Schaumann, G.E., Philippe, A., Bundschuh, M., Metreveli, G., Klitzke, S., Rakcheev, D., Grün, A.,
666 Kumahor, S.K., Kühn, M., Baumann, T., Lang, F., Manz, W., Schulz, R. and Vogel, H.J.,
667 2015. Understanding the fate and biological effects of Ag- and TiO<inf>2</inf>-
668 nanoparticles in the environment: The quest for advanced analytics and interdisciplinary
669 concepts. Science of The Total Environment, 535: 3-19.
670 Schilling, K., Bradford, B., Castelli, D., Dufour, E., Nash, J.F., Pape, W., Schulte, S., Tooley, I.,
671 van den Bosch, J. and Schellauf, F., 2010. Human safety review of "nano" titanium dioxide
672 and zinc oxide. Photochemical & Photobiological Sciences, 9(4): 495-509.
673 Shi, H., Magaye, R., Castranova, V. and Zhao, J., 2013. Titanium dioxide nanoparticles: a review of
674 current toxicological data. Particle and Fibre Toxicology, 10(1): 15.
675 Sim, Y. and Chrysikopoulos, C.V., 1998. Analytical solutions for solute transport in saturated
676 porous media with semi-infinite or finite thickness. Advances in Water Resources, 22(5):
677 507-519.
678 Sim, Y. and Chrysikopoulos, C.V., 1999. Analytical models for virus adsorption and inactivation in
679 unsaturated porous media. Colloids and Surfaces A: Physicochemical and Engineering
680 Aspects, 155(2–3): 189-197.
681 Šimůnek, J., Van Genuchten, M.T. and Šejna, M., 2008. Development and applications of the
682 HYDRUS and STANMOD software packages and related codes. Vadose Zone Journal,
683 7(2): 587-600.
684 Siripattanakul-Ratpukdi, S. and Fürhacker, M., 2014. Review: Issues of Silver Nanoparticles in
685 Engineered Environmental Treatment Systems. Water, Air, & Soil Pollution, 225(4): 1-18.
686 Sun, T.Y., Gottschalk, F., Hungerbühler, K. and Nowack, B., 2014. Comprehensive probabilistic
687 modelling of environmental emissions of engineered nanomaterials. Environmental
688 Pollution, 185(0): 69-76.
689 Tosco, T. and Sethi, R., 2009. MNM1D: a numerical code for colloid transport in porous media:
690 implementation and validation. American Journal of Environmental Sciences, 5(4): 517-525.
691 Tosco, T., Tiraferri, A. and Sethi, R., 2009. Ionic Strength Dependent Transport of Microparticles
692 in Saturated Porous Media: Modeling Mobilization and Immobilization Phenomena under
693 Transient Chemical Conditions. Environmental Science & Technology, 43(12): 4425-4431.
694 Tosco, T., Gastone, F. and Sethi, R., 2014. Guar gum solutions for improved delivery of iron
695 particles in porous media (Part 2): Iron transport tests and modeling in radial geometry.
696 Journal of Contaminant Hydrology, 166(0): 34-51.
697 Tufenkji, N. and Elimelech, M., 2004. Correlation Equation for Predicting Single-Collector
698 Efficiency in Physicochemical Filtration in Saturated Porous Media. Environmental Science
699 and Technology, 38(2): 529-536.
700 Varner, K.E., El-Badawy, A., Feldhake, D. and Venkatapathy, R., 2010. State-Of-The-Science
701 Review: Everything NanoSilver and More, U.S. Environmental Protection Agency,
702 Washington, DC.

Verginelli, I. and Baciocchi, R., 2013. Role of natural attenuation in modeling the leaching of contaminants in the risk analysis framework. Journal of Environmental Management, 114(0): 395-403.

Wang, D., Su, C., Zhang, W., Hao, X., Cang, L., Wang, Y. and Zhou, D., 2014. Laboratory assessment of the mobility of water-dispersed engineered nanoparticles in a red soil (Ultisol). Journal of Hydrology, 519, Part B(0): 1677-1687.

Werner, D., Karapanagioti, H.K. and Sabatini, D.A., 2012. Assessing the effect of grain-scale sorption rate limitations on the fate of hydrophobic organic groundwater pollutants. Journal of Contaminant Hydrology, 129–130(0): 70-79.

Westerhoff, P. and Nowack, B., 2012. Searching for Global Descriptors of Engineered Nanomaterial Fate and Transport in the Environment. Accounts of Chemical Research, 46(3): 844-853.

Windler, L., Height, M. and Nowack, B., 2013. Comparative evaluation of antimicrobials for textile applications. Environment International, 53(0): 62-73.

Yang, Y., Xu, M., Wall, J.D. and Hu, Z., 2012. Nanosilver impact on methanogenesis and biogas production from municipal solid waste. Waste Management, 32(5): 816-825.

Yao, K.-M., Habibian, M.T. and O'Melia, C.R., 1971. Water and waste water filtration. Concepts and applications. Environmental Science & Technology, 5(11): 1105-1112.

Figures

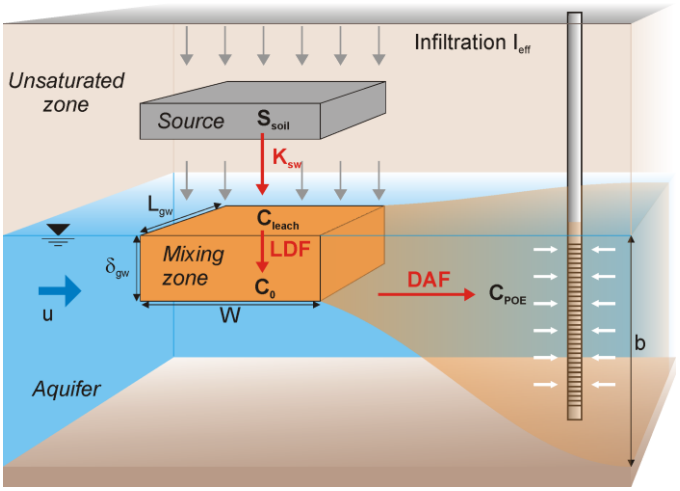

Figure 1: Scheme of particle release and transport.

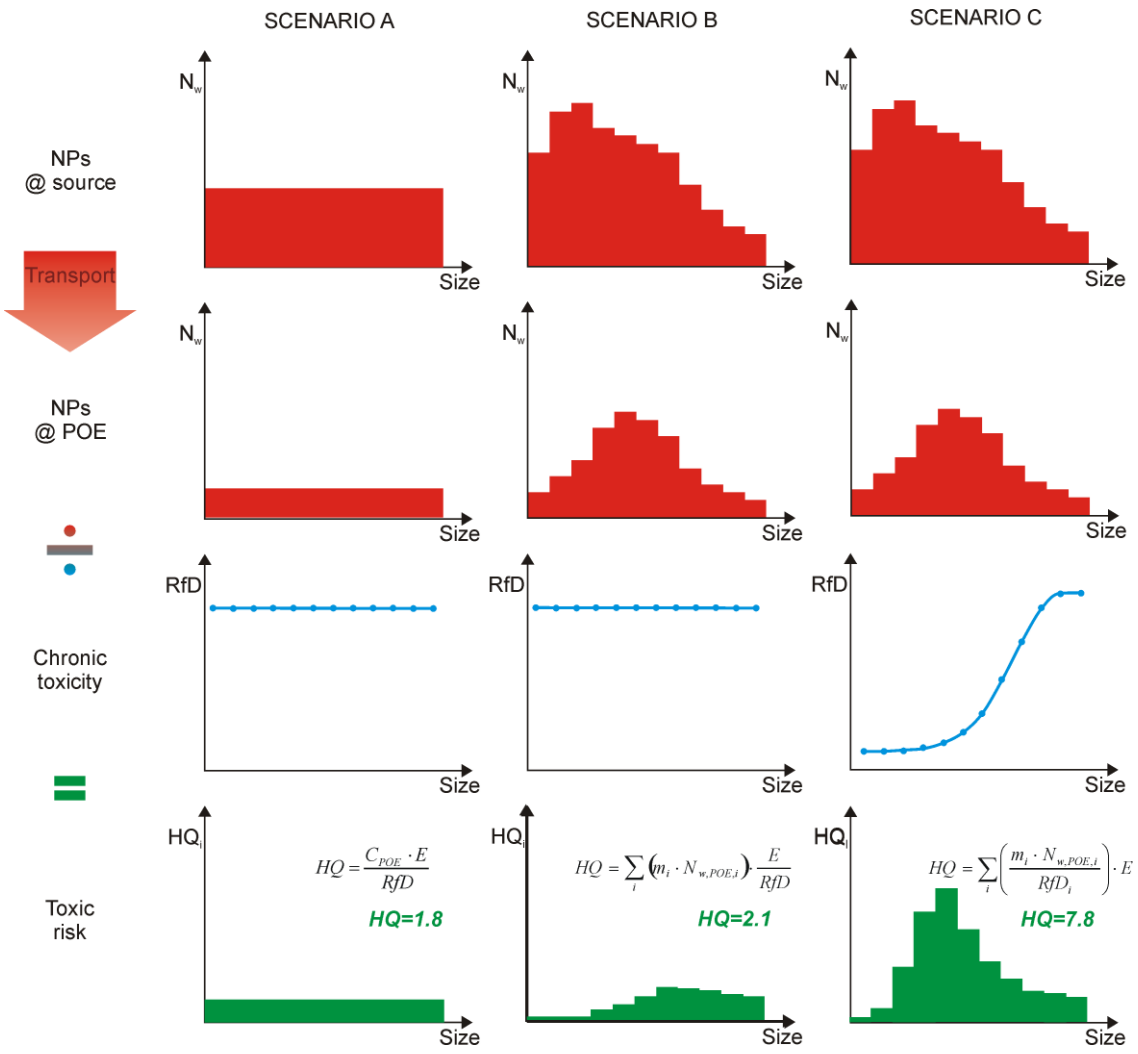

731

732 **Figure 2: Comparison of three different scenarios for the application of NP-adapted risk assessment procedure:**
733 **Scenario A, assuming no size-dependent transport nor toxicity; Scenario B, assuming size-dependent NP**
734 **transport; Scenario C, assuming size-dependent transport and toxicity. The released concentration is the same in**
735 **all scenarios.**

736

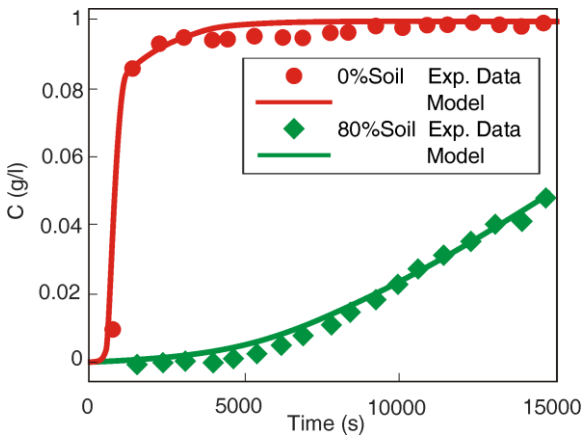

737

738 **Figure 3: Experimental and simulated Ag-NP breakthrough curves for the experimental data of Wang et al.**
739 **(2014) for 0%Soil and 80%Soil tests.**

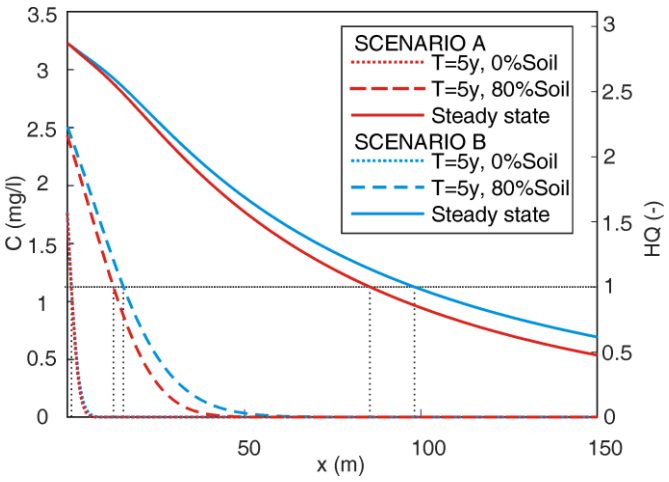

740

741 **Figure 4: Synthetic test case for Ag-NPs release from a landfill: simulated Ag-NPs concentrations in**
742 **groundwater and corresponding HQ values along the x axis (y=0, z=0) at steady state conditions (solid lines) and**
743 **in transient conditions after 5 years for 0%Soil (dashed lines) and 80%Soil (dotted lines) for Scenario A (red)**
744 **and Scenario B (blue).**

745

746

747

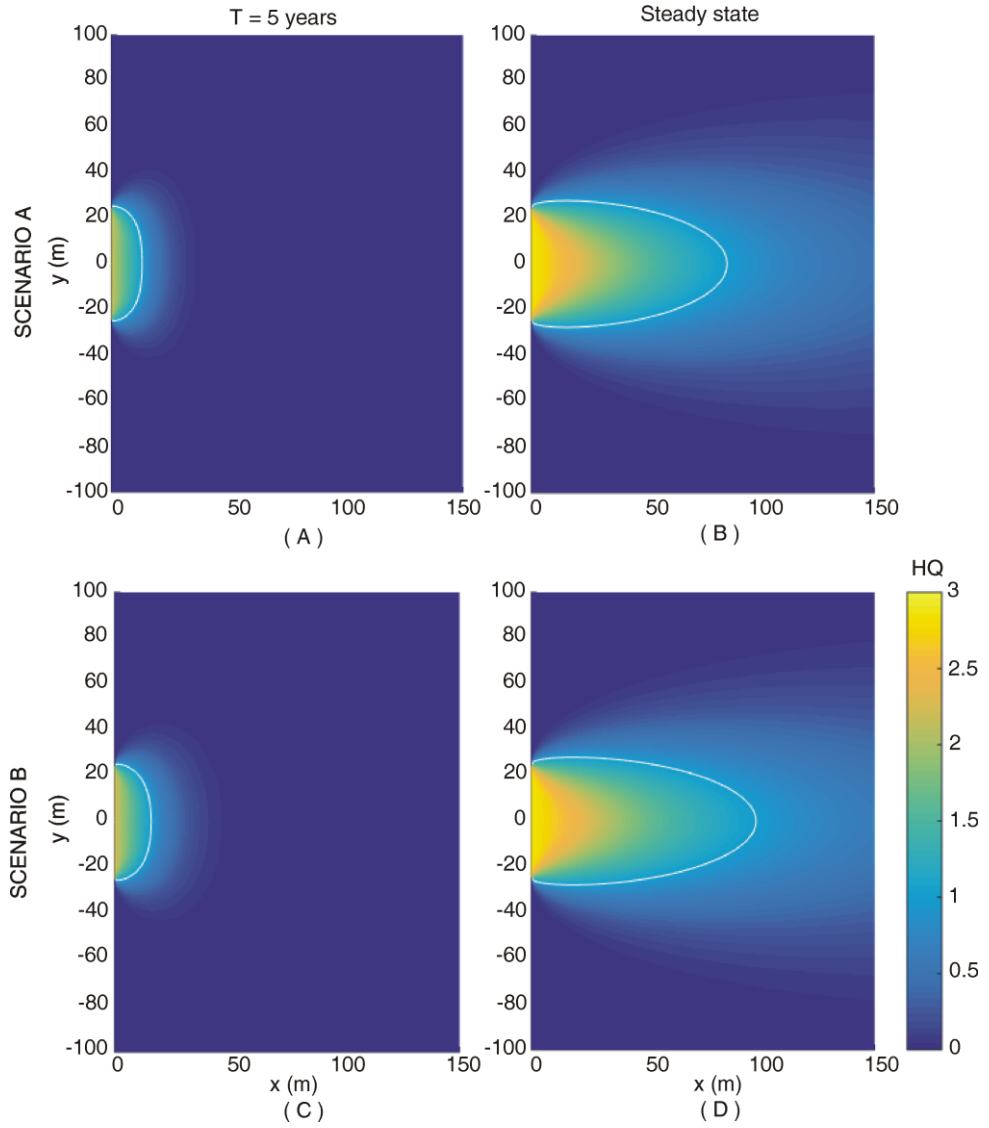

748

749 **Figure 5: HQ maps calculated applying transient Domenico's solution after 5 years (Eq. S.6) for 0%Soil (A-C),**
750 **and steady state solution (Eq. 6) (B-D). HQ is calculated assuming no size-dependent transport (A-B,**
751 **corresponding to Scenario A in Figure 2) and size-dependent transport (C-D, corresponding to Scenario B in**
752 **Figure 2).The white line corresponds to HQ=1.**

753

754

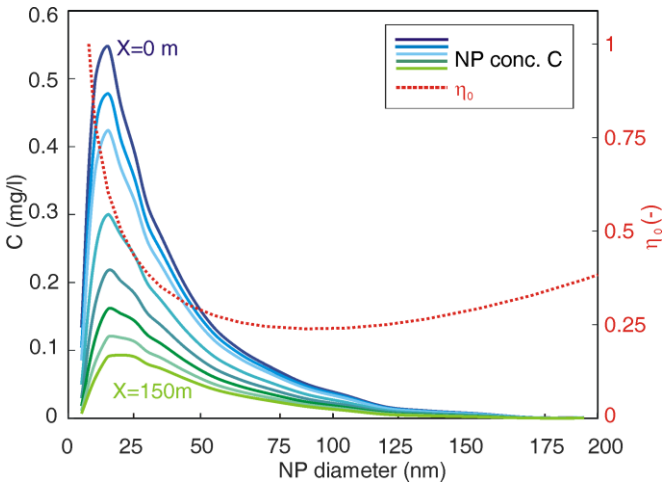

Figure 6: Synthetic test case for Ag-NPs release from a landfill: particle size distribution for Scenario B along the x axis y=0, z=0) at steady state, at different distances from the source (blue to green lines), and attachment efficiency as a function of particles size (red line).

Tables

Table 1: : Retention mechanisms for NP transport (1 or 2 interaction sites) and associated simplifying assumptions and parameter definition for the application of Domenico's solution

Retention mechanism(s)		Simplifying assumptions	Definition of Domenico's parameters	Applicability of Domenico's solution	
				Transient (Eq. S.6)	Steady state (Eq. 6)
1 site linear $\psi_i = 1$	Irreversible $k_{d,i} = 0$	None	$\lambda_i = \varepsilon k_{a,i}$ $R_i = 1$	Yes	Yes
	Reversible $k_{d,i} \neq 0$	$\frac{1}{K_{eq,i}} << \frac{x}{v}$	$\lambda_i = 0$ $R_i = 1 + \frac{k_{a,i}}{k_{d,i}}$	Yes	Yes
1 site blocking $\psi_i = 1 - \frac{N_{s,i}}{N_{s\max,i}}$	Any (reversible or irreversible)	$\frac{1}{K_{eq,i}} << \frac{x}{v}$	$\lambda_i = 0$ R_i n.d.	No	Yes
2 sites	Site 1: linear irrev. Site 2: linear rev.	$\frac{1}{K_{eq,i}} << \frac{x}{v}$	$\lambda_i = \varepsilon k_{a1,i}$ $R_i = 1 + \frac{k_{a2,i}}{k_{d2,i}}$	Yes	Yes
	Site 1: linear irrev. Site 2: blocking	$\frac{1}{K_{eq,i}} << \frac{x}{v}$	$\lambda_i = \varepsilon k_{a1,i}$ R_i n.d.	No	Yes
	J=1 linear rev. J=2 blocking	$\frac{1}{K_{eq,i}} << \frac{x}{v}$	$\lambda_i = 0$ R_i n.d.	No	Yes

Table 2: Transport parameters for NPs in column tests and for the test case of Ag-NP release from a landfill

Parameter	Column tests		Scenario A		Scenario B	
	0%Soil	80%Soil	0%Soil	80%Soil	0%Soil	80%Soil
Site 1						
Attachment rate k_{a1} (s^{-1})	$1.7 \cdot 10^{-7}$		$3.4 \cdot 10^{-8}$		$1.3 \cdot 10^{-8}$ - $7.0 \cdot 10^{-8}$	
Degradation rate $\lambda = \varepsilon \cdot k_{a1}$ (s^{-1})	$1.5 \cdot 10^{-8}$		$6.7 \cdot 10^{-9}$		$2.6 \cdot 10^{-9}$ - $1.4 \cdot 10^{-8}$	
Site 2						
Attachment rate k_{a2} (s^{-1})	$3.0 \cdot 10^{-4}$	$1.0 \cdot 10^{-2}$	$5.9 \cdot 10^{-5}$	$2.0 \cdot 10^{-3}$	$2.3 \cdot 10^{-5}$-$1.2 \cdot 10^{-4}$	$4.5 \cdot 10^{-3}$-$1.0 \cdot 10^{-2}$
Detachment rate k_{d2} (s^{-1})	$7.0 \cdot 10^{-4}$	$5.0 \cdot 10^{-4}$	$5.0 \cdot 10^{-6}$	$3.6 \cdot 10^{-6}$	$5.0 \cdot 10^{-6}$	$3.6 \cdot 10^{-6}$
Retardation coeff. R (-)	1.4	21.0	12.8	562.0	5.6-25.4	222-1160